A. Frisoli*
M. Solazzi
F. Salsedo
M. Bergamasco
PERCRO, Scuola Superiore
Sant'Anna
Viale Rinaldo Piaggio
Pisa, 56025 Italy

A Fingertip Haptic Display for Improving Curvature Discrimination

Abstract

This paper presents a novel haptic device providing both kinesthetic and cutaneous cues informative of shape geometry at the contact point. The system is composed of a supporting kinesthetic haptic interface and an innovative fingertip haptic display that can instantaneously orient a small plate along the tangent plane at the contact point with a virtual shape and bring it in contact with the fingertip. We show how this local augmentation of displayed haptic information can improve human performance in shape exploration, by assessing perception thresholds in curvature discrimination. When kinesthetic feedback was enriched with cutaneous cues, we found a significantly lower threshold for curvature discrimination ($1.51 \pm 0.2\ m^{-1}$ vs. $2.62 \pm 0.61\ m^{-1}$, $p < .05$) for stimuli constituted of spheres with curvature ranging in the interval from $4-6\ m^{-1}$. This confirms the importance in haptic perception of the stimulation of cutaneous mechanoreceptors at the fingertip.

1 Introduction

Haptic interaction allows a user to naturally perform both exploration and active manipulation of objects. Haptic perception by free exploration with bare fingers can provide accurate discrimination of shapes through both active proprioception and passive cutaneous mechanoreception (Lederman & Klatzky, 1987). While proprioception involves kinesthetic sense and is usually associated with an exploratory strategy of contour-following, cutaneous mechanoreception involves skin cutaneous receptors conducted under static contact with small exploratory movements and is more accurate in the judgment of shape.

In natural haptic exploration of real shapes, both curvature discrimination (Horst & Kappers, 2007) and object recognition (Jansson, Bergamasco, & Frisoli, 2003) are affected by the number of fingers. In particular, object recognition improves using multiple digits as opposed to one finger, but this holds only if the supplied cutaneous cues remain intact. Jansson et al. observed a significant deterioration in performance when only one finger was available for exploration of common objects with respect to when the same task was carried out with two or more fingers. But when the same experiment was conducted by attaching a hard sheath to the fingers in contact with the objects,

Presence, *Vol. 17, No. 6, December 2008,* 550–561

*Correspondence to a.frisoli@sssup.it.

the exploration time did not change between the one finger and two finger conditions (Jansson & Monaci, 2006). This suggests that geometric restrictions imposed at the fingertip contact region can blunt haptic perception, since physical properties of the contact surface (e.g., sliding conditions, friction, hardness, and local geometry) contribute to the perception of shape.

This hypothesis well explains the lack of improvement in perception with the number of fingers that was also observed in an experiment of simulated exploration of virtual shapes with a kinesthetic haptic device conducted by Frisoli, Wu, Ruffaldi, and Bergamasco (2005), in which no improvement in shape recognition was found with the number of contact points, from one to up to three fingers, measured in terms of proportions of correct answers and exploration time in contact with the virtual surface. Also in simulated active manipulation, such as precision grip of virtual objects mediated by a kinesthetic haptic interface, the amount of grip force exerted for lifting virtual objects was found to be higher than the grip force adopted for lifting real objects (Bergamasco, Avizzano, Frisoli, Ruffaldi, & Marcheschi, 2006). Several factors can account for the observed reduction in performance in these experiments, such as the lack of a physical contact location on the fingertip, and lack of geometrical information on the orientation, on the curvature of the contact area, and on the friction conditions. On this basis, several new conceptual schemes have been recently proposed to overcome these limitations. Some researchers have considered that shape recognition is influenced either by the perception of slipping the fingertip over an object's surface or by the change in contact area on the fingertip. It has been shown that relative motion and contact location can be used to render haptic sensation. Salada, Colgate, Lee, and Vishton (2002) showed with a prototype device in one degree of freedom that a rotating drum or sphere, used to render the velocity of a surface as it passes beneath the fingertip, is sufficient to create a haptic illusion of moving along a fixed, flat surface. Kuchenbecker, Provancher, Niemeyer, and Cutkosky (2004) used a rolling element in contact with the finger to display the location of the contact point of a virtual surface and found that contact location information significantly improves contour-following capabilities, reducing completion time and failure rate. Using the same device for the estimation of curvature, they also found that curvature discrimination is influenced by the display of contact location (Provancher, Cutkosky, Kuchenbecker, & Niemeyer, 2005). Scilingo, Sgambelluri, Tonietti, and Bicchi (2007) developed a new configuration for a haptic system that can simultaneously replicate independently the force/displacement and force/area profiles of a given material, while Magnenat-Thalmann et al. (2007) developed an integrated two-finger haptic system for the manipulation of textiles with integrated kinesthetic and tactile feedback.

Other studies suggest that shape recognition is linked to the perception of the orientation of the object's surface at the contact points. Early work in this direction included the surface display described by Hirota and Hirose (1993), while Yokokohji, Hollis, and Kanade (1999) and Yokokohji, Muramori, Sato, and Yoshikawa (2005) developed a robotic system that can orient mobile surfaces on the tangent planes to the simulated virtual object at the contact points with the finger. Among the local properties of the contact surface, curvature represents an important requisite to our perception of shape. Recently, Dostmohamed and Hayward (2005) demonstrated that curvature discrimination can be carried out through a device providing only surface orientation/slope cues at the fingertip, without any kinesthetic information and with a planar motion of the finger.

Following this research direction, in this article we investigate how curvature perception is influenced and how it can be enhanced during haptic exploration of shapes performed with haptic devices. We study the role of kinesthetic and cutaneous information in the perception of curvature and present the design of a new device that can enhance the perception of shape. The device can simultaneously provide both kinesthetic (force) and cutaneous (contact orientation) cues at the fingertip, and is composed of a supporting kinesthetic haptic interface and a haptic display for the fingertip. The fingertip haptic display can show the local orientation of the tangent plane to the virtual shape at the contact point by aligning an actuated mobile plate to the tangent

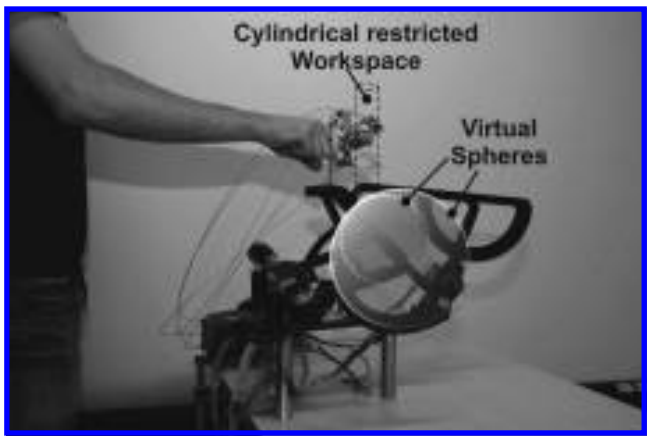

Figure 1. *Experimental setup with superimposed haptic cues displayed to the user.*

plane and putting the plate in contact with the fingertip. We show how the performance of curvature discrimination is significantly improved when cutaneous cues are displayed, compared with the case when only kinesthetic cues are presented. The remainder of the article is organized as follows. In Section 2 the overall device is presented with a description of the mechanical design and the adopted control strategy. In Section 3 psychophysical experiments investigating the role of cutaneous cues in the discrimination of curvature are reported, followed by conclusions in Section 4.

2 Description of the Haptic Interface

The system is composed of a fingertip haptic interface mounted on a kinesthetic haptic interface according to the overall configuration shown in Figure 1. The latter has the function of sustaining the weight of the fingertip device and tracking its position.

Figure 2 shows a conceptual scheme of the system. Suppose the user is interacting with a virtual object. When the finger is away from the surface of the object, the plate of the fingertip haptic interface is kept away from the fingertip. When the finger touches the virtual surface, the plate comes in contact with the fingertip with an orientation determined by the geometric normal to the explored surface. A reaction force proportional to the penetration is exerted simultaneously by the supporting kinesthetic haptic interface.

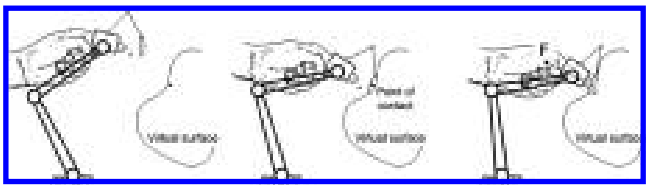

Figure 2. *The conceptual scheme of the device.*

2.1 The Supporting Haptic Interface

The supporting haptic interface is a pure translational parallel manipulator with three degrees of freedom (DOF). The system was developed through the redesign of an existing haptic interface (Frisoli, Sotgiu, Avizzano, Checcacci, & Bergamasco, 2004) which has led to a significant improvement of performance in terms of exertable forces, gravity auto-compensation capability, backlash, and constructive simplification. The end-effector is connected to the fixed base via three serial kinematic chains (legs) consisting of two links connected by an actuated revolute joint and two universal joints at the leg end. Figure 3 shows a diagram of the device kinematics with a representation of its reachable workspace. The reachable workspace is formed by the intersection of three spherical shells centered at the base universal joints with inner and outer radii determined by the minimum and maximum angles of the elbow joint of each leg.

The design of the device was optimized in order to minimize the friction forces and the inertia of the moving parts for the required transparency of the mechanism during haptic exploration. The actuation is realized by three brushed DC motors through a steel cable transmission, characterized by low friction and zero backlash as shown in Figure 4. The transmission system implements a speed reduction between the motor pulley and the actuated joint, allowing the motors to be mounted close to the base at the center of the first universal joint.

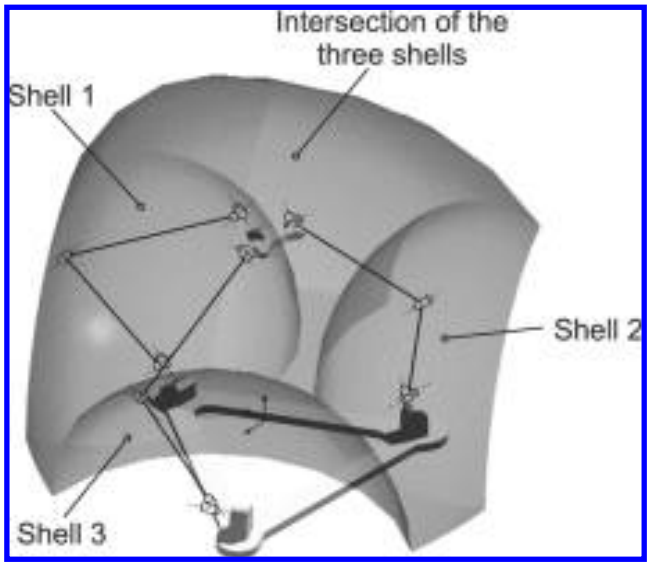

Figure 3. *Kinematics and reachable workspace of the supporting three DOF haptic device.*

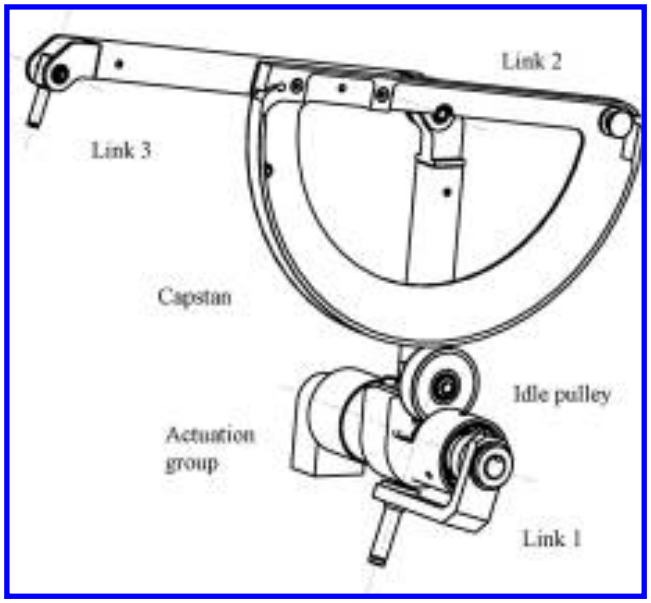

Figure 4. *CAD design of the leg of the supporting haptic device.*

As shown in Figure 4, the actuation group was specifically designed to place its center of gravity at the intersection of the first two joint axes of each leg. Since this property holds in every configuration, the gravity force due to weight of the overall actuation group, applied at its center of mass, does not exert any moment on the first two passive joints of each leg. As a consequence of this design, the weight of the actuation group is statically self-balanced in any configuration and a passive gravity compensation of the mechanism is achieved, except for the upper platform, with the effect of reducing the inertia perceived at the end-effector. The maximum force that could be exerted at the end-effector is also increased since the motors are required to actively compensate for only the weight of the upper platform.

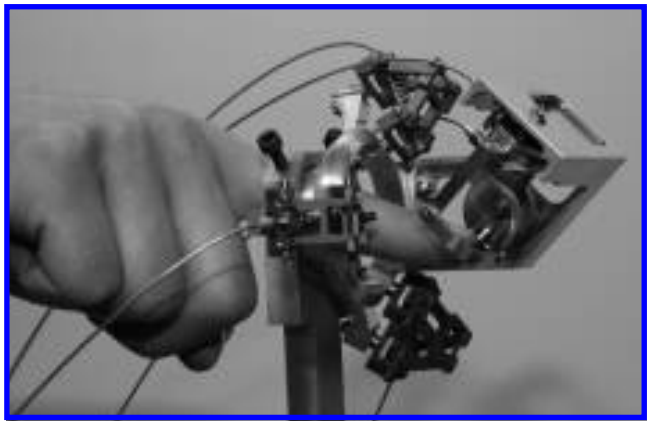

Figure 5. *The fingertip haptic interface.*

2.2 The Fingertip Haptic Interface

The fingertip haptic interface was devised to bring the final plate into contact with the fingertip at different orientations defined by the normal to the virtual surface at the point of contact (Cini, Frisoli, Marcheschi, Salsedo, & Bergamasco, 2005). The contact can occur at different points of the fingertip surface depending on its orientation with respect to the virtual surface. These requirements can be satisfied by a kinematics with five DOF—three that are translational and two rotational. Our most suitable solution resulted in a decoupled kinematics consisting of a parallel rotational stage and a parallel translational stage. The overall device is shown in Figure 5.

The kinematics and the CAD model of the rotational

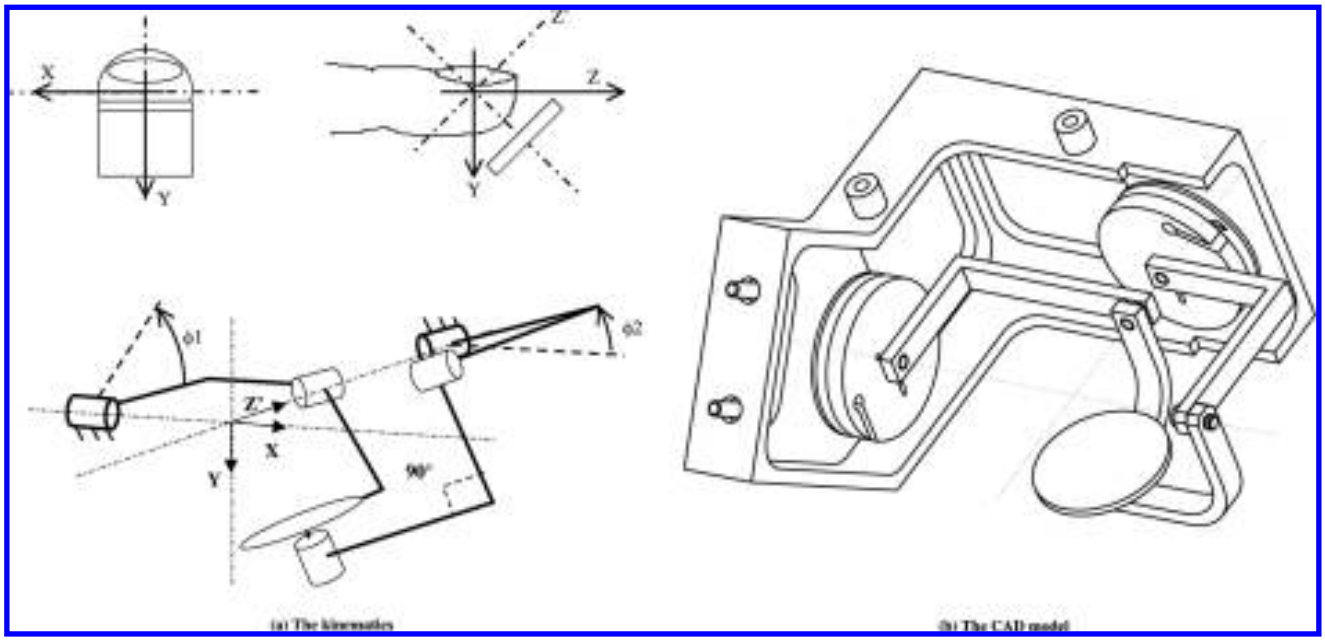

Figure 6. *The rotational stage of the device. (a) The kinematics. (b) The CAD model.*

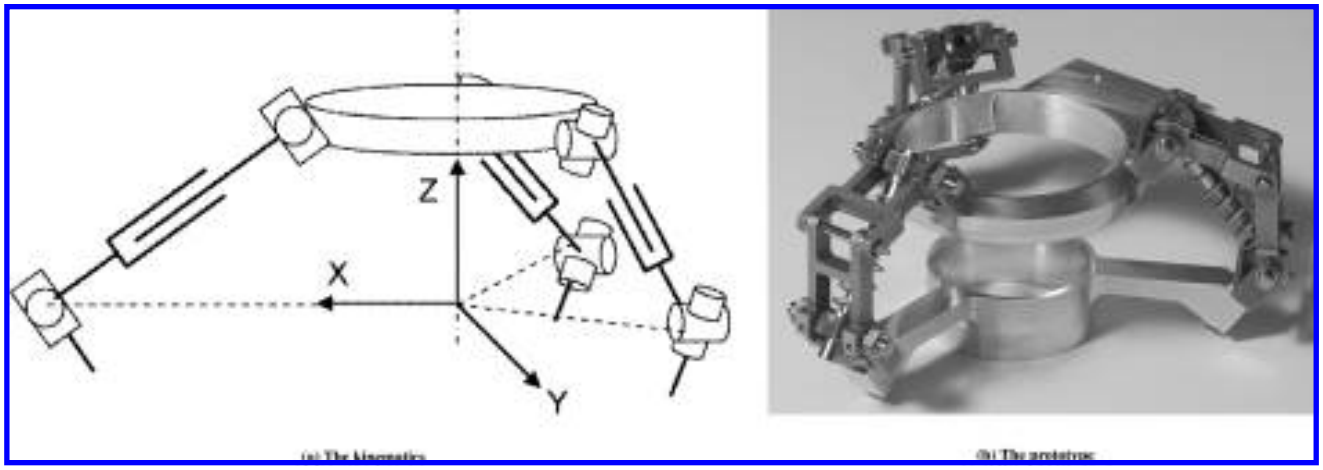

Figure 7. *The translational stage of the device. (a) The kinematics. (b) The prototype.*

stage are shown in Figure 6; the axes of rotation X and Z' are fixed to the translational stage and allow a rotation of 90° and 180° respectively.

The translational stage (Figure 7) has the same kinematics of the supporting haptic interface with three legs consisting of two links connected by a revolute joint and two universal joints at the leg end.

The overall device is actuated by five DC motors placed on a fixed external support in order to reduce the mass and the bulk of the moving structure. This is achieved with a transmission system using steel cables guided by flexible sheaths that begin at the actuation group and reach the driven joints. As is shown in Figure 8 for the case of one leg of the translational stage, the

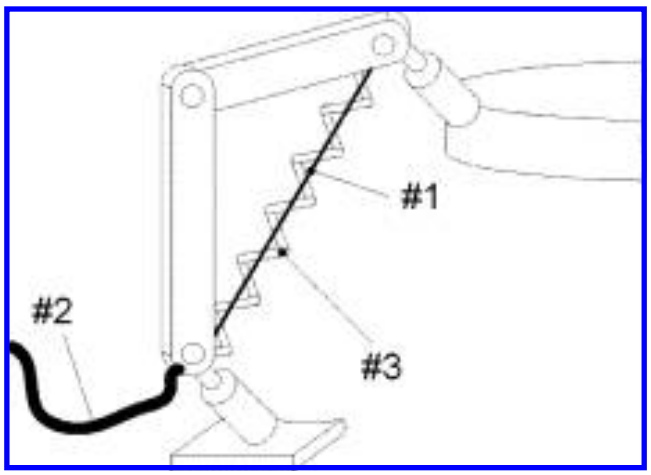

Figure 8. *The actuation of one leg of the translation stage.*

actuation cable (#1), connected to the motor through a flexible sheath (#2), works in opposition with a compression spring (#3) that is mounted aligned to the centers of the universal joints and can guarantee the needed preload on the cable.

2.3 The Control Architecture

Figure 9 shows a diagram of the actuation system of one joint of the fingertip interface composed of the actuation cable (#1), the flexible sheath (#2), the return spring (#3), the motor (#4), and the load representing the equivalent mass after the joint (#5).

According to the notation of Figure 9, the dynamic equations of the motor for each leg can be written as follows:

$$\begin{cases} \tau_m - T_{in} r = J_m \ddot{\theta} + b_m \dot{\theta}, \\ T_{out} = r[K_m(\theta - \theta_0) + m\ddot{\theta}] + T_g \end{cases} \quad (1)$$

where τ_m is the motor torque, r is the motor pulley radius, J_m and b_m are respectively the motor inertia and damping constant, T_{in} and T_{out} are the cable tension, respectively, at the entry and exit of the sheath, K_m the stiffness of the return spring, θ_0 the equivalent length at rest of the return spring, and T_g the feed-forward requested torque that is applied to balance the weight of the device.

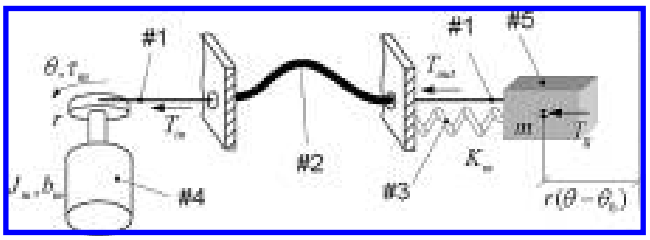

Figure 9. *Scheme of the joint actuation.*

The friction of the sheath was modeled according to the theory of belts with the efficiency μ of the transmission expressed as $\mu = e^{f\beta} - 1$, where β and f represent, respectively, the winding angle of the tendon on the pulley and the friction coefficient between the groove and the cable, and with a viscous dissipation term expressed by a damping factor b. The relation $\Gamma(\cdot)$ between T_{in} and T_{out} was determined according to the drive of motion, either by the motor or by the return spring:

$$T_{in} = \Gamma(T_{out}),$$

$$\Gamma: \begin{cases} T_{in} = T_{out}(1 + \mu) + b\dot{\theta} = T_{out}e^{f\beta} + b\dot{\theta}, \\ \quad \text{if } \dot{\theta} > 0, \text{ motor drive} \\ T_{in} = \dfrac{T_{out}}{(1 + \mu)} + b\dot{\theta} = \dfrac{T_{out}}{e^{f\beta}} + b\dot{\theta}, \\ \quad \text{if } \dot{\theta} < 0, \text{ return spring drive} \end{cases} \quad (2)$$

The unknown friction coefficients between the steel cable and the sheath were identified in different geometric configurations, that is, for different curvature radii, through an experimental apparatus which allows the application of a constant tension to the steel cable running inside the sheath. The experimental apparatus consisted of a position-controlled DC motor connected to a sheathed cable with a given curvature through a motor pulley, on which the cable had been wound. On the other side of the sheathed tendon, a weight of known mass was suspended and allowed to move. The motor was then used to lift up the weight, at constant cable tension and with different speeds, and the friction coefficients were experimentally estimated according to the motor currents required for different cable tensions and velocities.

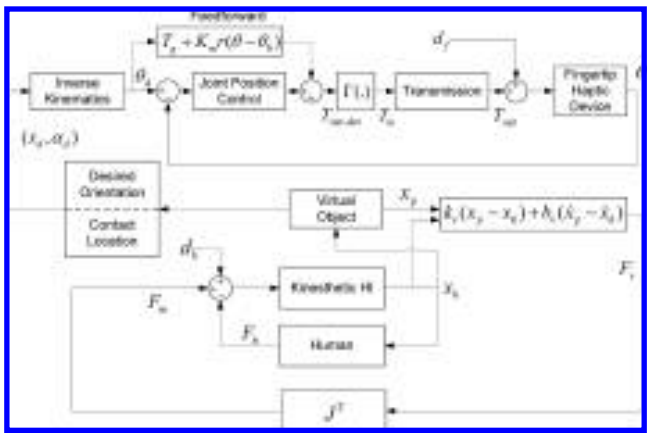

Figure 10. *Control architecture.*

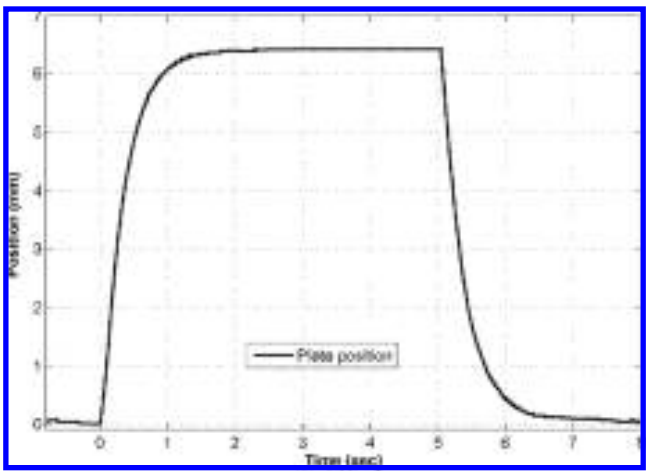

Figure 11. *Experimental step response of the fingertip device during the contact phase.*

The overall control architecture is shown in Figure 10.

In order to render the contact with a virtual shape, the position of a proxy point x_p was calculated as the closest point on the virtual surface to the haptic interface point x_h, when x_h is inside the shape. The kinesthetic haptic interface was controlled according to a classic impedance control scheme (Carignan & Cleary, 2000), generating a force F_v depending on the penetration into the virtual surface $(x_p - x_h)$ with stiffness k_v and damping b_u. The force F_v was then converted into motor torques F_m through the static Jacobian of the system J^T. The force F_h represents the effect of the human operator.

The control of the fingertip haptic device was implemented with joint position controllers. The plate was controlled in order to maintain it at a given distance from the finger when there was no contact with the virtual surface, and to move it into contact with the finger during the contact phase. According to the relative position of the haptic interface point x_h with respect to the virtual shape, a desired orientation and contact location of the plate was calculated from the position x_d and orientation α_d of the plate. An inverse kinematics module was used to convert the position x_d and orientation α_d to the corresponding joint coordinates θ_d. The nonlinear terms due to the spring preload $K_m r(\theta - \theta_0)$ and the gravity term T_g were precompensated in feedforward, while Equation 2 was used to compensate through the function $\Gamma(\cdot)$ the nonlinearities due to the sheathed cable transmission.

Disturbance is modeled in Figure 10 by the parameters d_f and d_k, representing the disturbances introduced by the fingertip at the contact with the plate and the unmodeled effects of the human, respectively.

The step response of the fingertip device during the simulation of contact is shown in Figure 11, measured in the reference system solidal to the base of the fingertip device (see Figure 7) as the distance covered by the plate along the radial direction of the cylinder. When the software detects that the user is approaching the surface, the fingertip haptic interface is activated in advance in order to compensate for the response time needed to reach the finger, so that a simultaneous response of the fingertip and kinesthetic haptic interfaces can be achieved.

Figure 12 shows the position and the interaction forces evaluated by the currents supplied through the actuators during the contact with a virtual cylinder of radius 70 mm. The solid line and the dashed line in the top plot represent, respectively, the position of the plate and the finger (position of the supporting device), expressed in a set of polar coordinates as the distance to the cylinder axis. When the finger is out of the cylinder (values greater than 70 mm), the plate is moved away from the finger by a given offset. When the finger

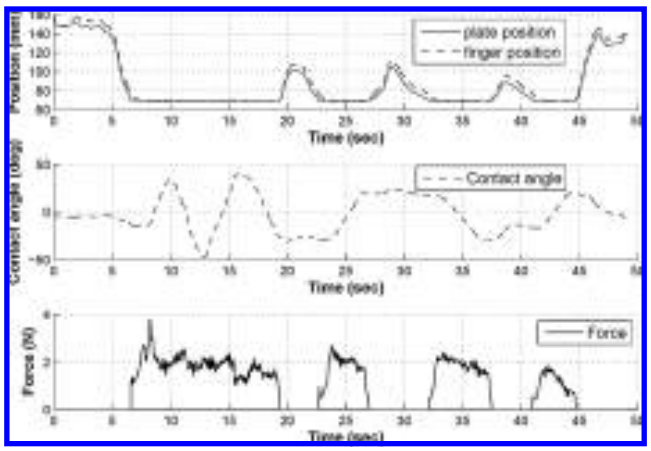

Figure 12. *Experimental plot showing the combined response of the two devices.*

comes in contact with the cylinder (values equal to 70 mm), the two positions coincide meaning that the plate is in contact with the finger. The black solid line in the bottom plot is a representation of force F_v generated by the supporting kinesthetic interface. The force is null when the finger is outside the cylinder. The fingertip device is always kept oriented according to the surface normal at the closest surface point to the haptic interface point x_h. The middle plot shows how the contact angle α_d is varied during the exploration by the finger of the surface of a cylinder. Once in contact with the surface ($F_v^y > 0$), the user begins to move the finger on the cylinder in the range of motion of $\pm 50°$ (dashed line).

3 Can Cutaneous Cues Improve Shape Perception?

An experiment was carried out in order to assess expected improvements in shape recognition due to the addition of cutaneous cues displayed through the new fingertip device. On the basis of the evidence demonstrated by Dostmohamed and Hayward (2005) in the perception of curvatures with a similar device, and due to the availability of data from previous experiments with real objects, an experiment on haptic discrimination of curvature was carried out. The aim of the test was to evaluate the difference threshold for curvature discrimination when both kinesthetic and cutaneous cues were available (condition A) and when only kinesthetic cues were available (condition B). The analysis of discrimination data was based on signal detection theory (TSD; Macmillan & Creelman, 1991).

3.1 Methods and Procedures

The same-different procedure of TSD (Gescheider, 1997) was implemented to evaluate the just noticeable difference (JND) for curvature. According to the signal detection theory, signals are detected by humans against a noisy background. Two probability distributions describe the variations in the noise (N) and the signal plus noise (SN). Each observer sets a criterion as a cutoff point for deciding if an observation belongs to noise or to signal plus noise. The proportion of "yes" responses for the SN distribution is called the hit rate, while the proportion of "yes" responses for the N distribution is the false alarm rate. In traditional psychophysical methods, only the hit rate is taken into account and it is possible that data from two subjects with the same sensitivity but different criteria will result in different thresholds. In TSD a sensitivity index d' is defined as the difference between the means of the SN and the N distributions, divided by the standard deviation of the N distribution. The value of d' represents the normalized separation between the SN and N distributions. Since d' depends only on stimulus intensity and properties of the sensory system but not on the observer's response criterion, it is generally assumed to be an uncontaminated index of detectability for a certain stimulus. In practice the value of d' can be calculated from the false alarm and hit rates after converting them to z scores.

Four participants, three males and one female, were recruited for the experiment. All were right handed. They were complete novices to haptic interfaces and did not have any dysfunction of the fingers. Each participant was informed about the procedure before the beginning of the experiment. Participants stood blindfolded in

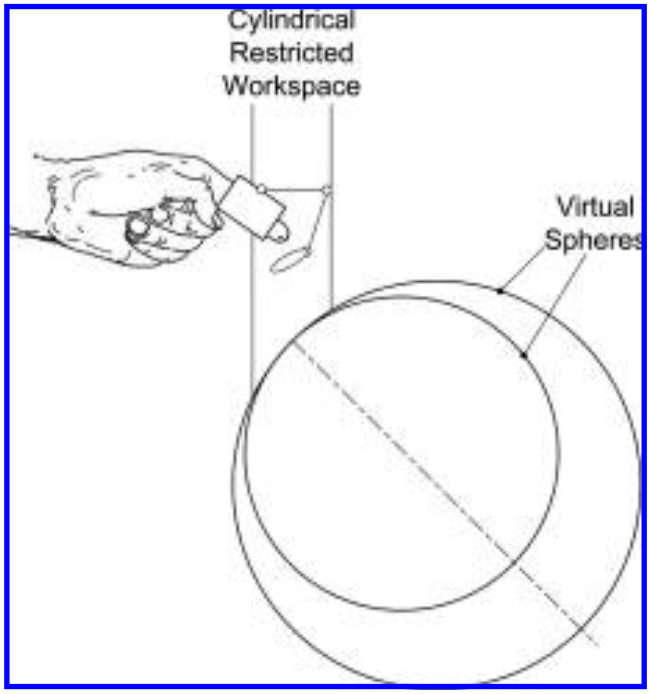

Figure 13. *Representation of the cues haptically displayed to the user.*

front of the device with a support for the elbow and were instructed to use the device with the right index finger to explore the surface of a virtual sphere. To avoid biases due to different orientations, our stimuli surfaces were made of spheres with uniform curvature in all directions.

According to the same-different procedure, each trial involved exploring in succession a pair of spheres in the virtual environment. The exploration was carried out in a restricted workspace consisting of a vertical cylinder with a diameter of 25 mm. Figure 13 shows the displayed haptic cues in a planar section, while Figure 1 shows their relative position and size with respect to the device.

There were two experimental conditions. In condition A, the mobile platform of the fingertip device was kept in contact with the fingertip when the user was in contact with the surface, with an orientation tangent to the displayed virtual surface. As a result the observer perceived the indentation of the platform at the contact point, oriented along the direction of the normal force applied by the kinesthetic device. In condition B, the mobile platform was substituted by a fixed thimble, into which the user was required to insert his or her finger. In this case the only haptic cue applied to the fingertip was the force perpendicular to the virtual surface generated by the supporting kinesthetic haptic interface; no local geometry information was provided.

Table 1. *Values of Presented Curvatures*

	Curvatures κ_a/κ_b	$\Delta\kappa$
Series 1	5 m^{-1}/6 m^{-1}	1 m^{-1}
Series 2	4.5 m^{-1}/6 m^{-1}	1.5 m^{-1}
Series 3	4 m^{-1}/6 m^{-1}	2 m^{-1}

The experiment consisted of three series of 100 trials. In each series two spheres with curvatures κ_a and κ_b were presented in random order. On each trial the participant had the same a priori probability of 0.5 to explore a pair of spheres with the same radius (κ_a,κ_a or κ_b,κ_b) or with different radii (κ_a,κ_b or κ_b,κ_a). The observer's task was to judge on each trial if the curvature of the two surfaces was different or the same. The order of presentation of the sequence of series for the two conditions was different for each subject in order to minimize learning effects. Three series with different values of $\Delta\kappa = \kappa_b - \kappa_a$ were presented to each participant (see Table 1).

3.2 Data Analysis

For each series, the data were arranged in a two-by-two stimulus-response matrix and the hit rate p_h and the false alarm rate p_f were calculated. The hit rate p_h corresponds to the percentage of correct responses given by the subject ("different") when the two surfaces of the pair had different curvatures (κ_a,κ_b or κ_b,κ_a), while the false alarm rate p_f corresponds to the percentage of incorrect responses ("different") when the curvatures of the two surfaces were the same (κ_a,κ_a or κ_b,κ_b). The rates p_h and p_f were

Table 2. *JND and Standard Deviation (SD) Values for All Subjects Between the Values of* d′ *and the Stimulus Difference* $\Delta\kappa$

	JND (m^{-1}) in condition A: cutaneous and kinesthetic cues	JND (m^{-1}) in condition B: only kinesthetic cues
Subject 1	1.61	2.72
Subject 2	1.37	1.76
Subject 3	1.73	2.78
Subject 4	1.31	3.22
Average	1.51	2.62
SD	0.2	0.61

converted to z score of the normal distribution, Z_h and Z_f, respectively.

Next, the sensitivity index d' was calculated as the difference between the two z scores:

$$d' = Z_h - Z_f \quad (3)$$

For each value of the three increments $\Delta\kappa$, the sensitivity measure d' was computed. According to the criterion commonly adopted in similar studies (Tan, Srinivasan, Reed, & Durlach, 2007; Pang, Tan, & Durlach, 1991; Gescheider, 1997), the just noticeable difference (JND) was defined as the difference between the curvatures for which d' is equal to 1. It was computed for each subject from the linear interpolating function in the least-square error sense using the three experimental points, assuming a proportionality between the values of d' and the stimulus difference $\Delta\kappa$. The overall JND was defined as the mean of the values obtained for all participants.

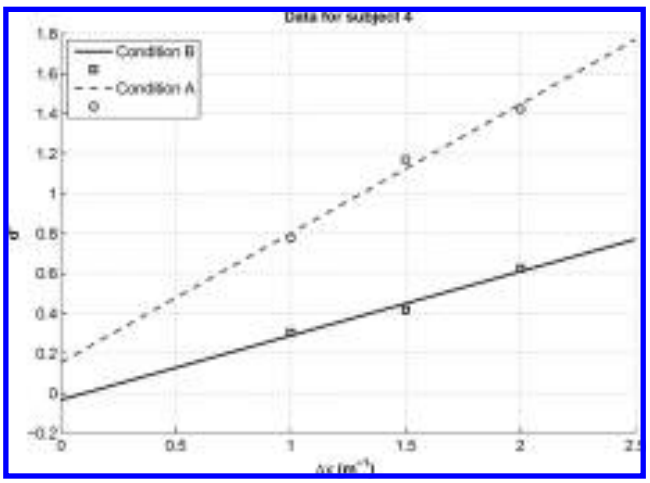

Figure 14. *Results for the fourth participant.*

3.3 Results and Discussion

The data obtained for the four subjects are shown in Table 2.

As an example, Figure 14 shows the sensitivity measure d' for the three $\Delta\kappa$ values and the interpolating lines for subject 4 in condition A (dashed line) and B (solid line). The plot confirms the hypothesis of proportionality.

The average JND values were significantly lower for condition A than for B as expected ($p < .05$, paired sampled t-test), with an average of 1.51 ± 0.2 m^{-1} and 2.62 ± 0.61 m^{-1} for conditions A and B, respectively, for curvatures ranging in the interval $4-6$ m^{-1}. Figure 15 shows a bar plot of the performance in the two conditions with error bars indicating ± 2 *SD*.

3.4 Discussion

Discrimination of curvature has been demonstrated to be related to the change of local surface attitude (slope) over the stimulus surface (Pont, Kappers, & Koenderink, 1999). For the subjects enrolled in the present experiment, we found a significant improvement in the curvature discrimination threshold

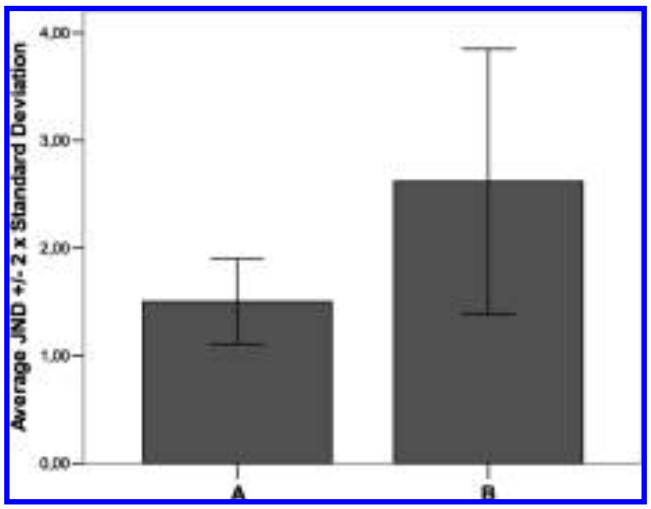

Figure 15. *Bar plot of performance in conditions A and B.*

when the subjects were provided with haptic cues informative of the local geometry at the contact point through the new device. The subjects commented that the additional cutaneous cues made the discrimination of curvature easier.

The observed discrimination threshold for curvature with only kinesthetic cues is in agreement with previous results in the literature. Henriques and Soechting (2003) found a similar value for curvature discrimination threshold by employing a two-joint robot arm: for a reference arc of 2.50 m^{-1}, they estimated a curvature discrimination threshold of 2.61 m^{-1} at a 50% correct performance level. Jansson (2002) found, using the method of limits, a curvature discrimination threshold of 1.11 m^{-1} for stimuli consisting of virtual spheres displayed by means of a SensAble PHANToM 1.5A haptic interface, for a reference curvature of 22.2 m^{-1}. Provancher et al. (2005) found discrimination thresholds of 3.58 m^{-1} and 2.6 m^{-1} for direct and virtual discrimination of spheres, respectively, with a reference curvature of 25 m^{-1}, with a better performance of virtual vs. real exploration for spheres with radii greater than 30 mm. In another study using real objects and a reference stimulus of 33 m^{-1}, Horst and Kappers (2006) found the curvature discrimination threshold for the index finger of the preferred hand to be about 2.5 m^{-1}, which was in general agreement with our findings. This is consistent with the observation that dynamic curvature discrimination of cylindrical surfaces does not follow Weber's law (Kappers & Koenderink, 1996), and a subject's performance improves with larger curvatures.

These data confirm that the display of surface orientation can aid haptic perception of shape (Dostmohamed & Hayward, 2005). Results obtained from the present study indicate that haptic shape perception can be compromised by the absence of local contact information and therefore explain the significant deterioration in perception observed in virtual exploration of shapes through kinesthetic haptic devices alone.

4 Conclusions and Future Work

In this article we have presented a novel concept of haptic interface based on the combination of a fingertip and a kinesthetic haptic interface that can provide both cutaneous and kinesthetic cues. This configuration can enhance human shape perception, as demonstrated by the observed improvement in curvature discrimination threshold. Future work foresees an evolution of this device for improved portability and reduced dimensions and an investigation of the effects of cutaneous cues alone without kinesthetic feedback.

Acknowledgments

The authors would like to thank all the involved reviewers and Associate Editor Prof. Hong Tan for their helpful and valuable comments. This work was carried out as part of the PRESENCCIA project, an EU funded Integrated Project under the IST programme (Project Number 27731).

References

Bergamasco, M., Avizzano, C., Frisoli, A., Ruffaldi, E., & Marcheschi, S. (2006). Design and validation of a complete haptic system for manipulative tasks. *Advanced Robotics, 20*(3), 367–389.

Carignan, C., & Cleary, K. (2000). Closed-loop force control for haptic simulation of virtual environments. *Haptics-e, 1*(2), 1–14.

Cini, G., Frisoli, A., Marcheschi, S., Salsedo, F., & Bergamasco, M. (2005). A novel fingertip haptic device for display of local contact geometry. *Proceedings of WorldHaptics, First Joint Eurohaptics Conference and IEEE Symposium on Haptic Interfaces for Virtual Environments and Teleoperator Systems,* 602–605.

Dostmohamed, H., & Hayward, V. (2005). Trajectory of contact region on the fingerpad gives the illusion of haptic shape. *Experimental Brain Research, 164*(3), 387–394.

Frisoli, A., Sotgiu, E., Avizzano, C., Checcacci, D., & Bergamasco, M. (2004). Force-based impedance control of a haptic master system for teleoperation. *Sensor Review, 24*(1), 42–50.

Frisoli, A., Wu, S., Ruffaldi, E., & Bergamasco, M. (2005). Evaluation of multipoint contact interfaces in haptic perception of shapes. In K. S. F. Barbagli & D. Prattichizzo (Eds.), *Multipoint interaction with real and virtual objects: Vol. 18. Springer Tracts in Advanced Robotics.* Berlin: Springer.

Gescheider, G. (1997). *Psychophysics: The fundamentals.* Mahwah, NJ: Lawrence Erlbaum.

Henriques, D., & Soechting, J. (2003). Bias and sensitivity in the haptic perception of geometry. *Experimental Brain Research, 150*(1), 95–108.

Hirota, K., & Hirose, M. (1993). Development of surface display. *Proceedings of the IEEE Virtual Reality Annual International Symposium,* 256–262.

Horst, B. Van der, & Kappers, A. (2007). Curvature discrimination in various finger conditions. *Experimental Brain Research, 17,* 304–311.

Jansson, G. (2002). *Pure-form deliverable d6: "Haptic exploration for perception of the shape of virtual objects"* (Tech. Rep.). Upssala University.

Jansson, G., Bergamasco, M., & Frisoli, A. (2003). A new option for the visually impaired to experience 3D art at museums: Manual exploration of virtual copies. *Visual Impairment Research, 5,* 1–12.

Jansson, G., & Monaci, L. (2006). Identification of real objects under conditions similar to those in haptic displays: Providing spatially distributed information at the contact areas is more important than increasing the number of areas. *Virtual Reality, 9*(4), 243–249.

Kappers, A., & Koenderink, J. (1996). Haptic unilateral and bilateral discrimination of curved surfaces. *Perception, 25*(6), 739–749.

Kuchenbecker, K. J., Provancher, W. R., Niemeyer, G., & Cutkosky, M. R. (2004). Haptic display of contact location. *Proceedings of the Symposium on Haptic Interfaces for Virtual Environment and Teleoperator Systems.*

Lederman, S., & Klatzky, R. (1987). Hand movements: A window into haptic object recognition. *Cognitive Psychology, 19*(3), 342–368.

Macmillan, N., & Creelman, C. (1991). *Detection theory: A user's guide.* Cambridge, UK: Cambridge University Press.

Magnenat-Thalmann, N., Volino, P., Bonanni, U., Summers, I. R., Bergamasco, M., Salsedo, F., et al. (2007). From physics-based simulation to the touching of textiles: The haptex project. *The International Journal of Virtual Reality, 6*(3), 35–44.

Pang, X., Tan, H., & Durlach, N. (1991). Manual discrimination of force using active finger motion. *Perception and Psychophysics, 49*(6), 531–540.

Pont, S., Kappers, A., & Koenderink, J. (1999). Similar mechanisms underlie curvature comparison by static and dynamic touch. *Perceptional Psychophysics, 61*(5), 874–894.

Provancher, W., Cutkosky, M., Kuchenbecker, K., & Niemeyer, G. (2005). Contact location display for haptic perception of curvature and object motion. *The International Journal of Robotics Research, 24*(9), 691.

Salada, M. A., Colgate, J. E., Lee, M. V., & Vishton, P. M. (2002). Validating a novel approach to rendering fingertip contact sensations. *Proceedings of the 10th IEEE Virtual Reality Haptics Symposium,* 217–224.

Scilingo, E., Sgambelluri, N., Tonietti, G., & Bicchi, A. (2007). Integrating two haptic devices for performance enhancement. *EuroHaptics Conference, 2007, Symposium on Haptic Interfaces for Virtual Environment and Teleoperator Systems. World Haptics 2007,* 139–144.

Tan, H., Srinivasan, M., Reed, C., & Durlach, N. (2007). Discrimination and identification of finger joint-angle position using active motion. *ACM Transactions on Applied Perception, 4*(2).

Yokokohji, Y., Hollis, R., & Kanade, T. (1999). WYSIWYF display: A visual/haptic interface to virtual environment. *Presence: Teleoperators and Virtual Environments, 8*(4), 412–434.

Yokokohji, Y., Muramori, N., Sato, Y., & Yoshikawa, T. (2005). Designing an encountered-type haptic display for multiple fingertip contacts based on the observation of human grasping behaviors. *The International Journal of Robotics Research, 24*(9), 717.